ACS Catalysis

Letter

pubs.acs.org/acscatalysis

Catalytic Epoxidation Reaction over N-Containing sp^2 Carbon Catalysts

Wenjing Li,[†] Yongjun Gao,[†] Wulin Chen,[‡] Pei Tang,[†] Weizhen Li,[†] Zujin Shi,[†] DangSheng Su,[§] Jianguo Wang,*[,‡] and Ding Ma*[,†]

[†]Beijing National Laboratory for Molecular Sciences, College of Chemistry and Molecular Engineering, Peking University, Beijing 100871, China

[‡]College of Chemical Engineering and Materials Science, Zhejiang University of Technology, Hangzhou 310032, China

[§]Shenyang National Laboratory for Materials Science, Institute of Metal Research, Chinese Academy of Science, 72 Wenhua Road, Shenyang 110016, China

Supporting Information

ABSTRACT: Nitrogen-doped graphene treated with ammonia under different temperatures was used as the catalysts for the epoxidation of *trans*-stilbene and styrene at 373 K. NG-800 (N-doped graphene treated at 800 °C for 8 h) performed the best and gave the highest recyclable catalytic activity for the epoxidation of *trans*-stilbene, with 95.8% conversion and 94.4% selectivity to *trans*-stilbene epoxide. The catalytic center has been identified with the reaction mechanism elucidated by DFT calculation.

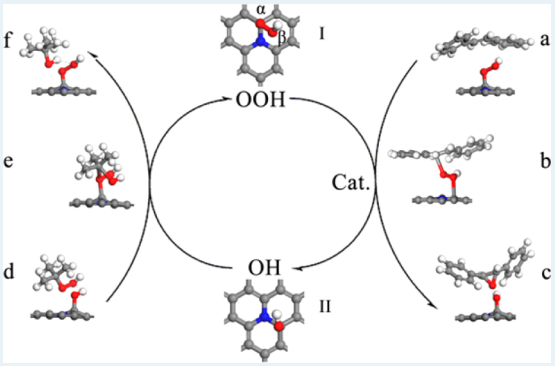

KEYWORDS: *nitrogen-doped graphene, carbon catalyst, trans-stilbene, epoxidation, DFT calculation*

Alkene epoxidation is an important industrial process because the products of the reactions, epoxides, are versatile intermediates in fine chemical synthesis. They serve as building blocks for the fabrication of plasticizers, perfumes, and pharmaceutical products.[1] Traditionally, the oxianes were obtained by the direct oxidation of alkenes with stoichiometric peracids,[2] which produced large amounts of waste and byproducts. Even worse, the peracids were unsafe and corrosive to the equipments used in the process. With growing attention paid to the environmental issue, much more effort was made to develop a variety of new processes for the epoxidation reactions by using different environmentally benign oxidants, such as TBHP,[3,4] H_2O_2,[1,5−7] oxygen,[8] and air.[9] It has been reported that when TBHP was used as the oxidizing agent for alkene epoxidation, supported gold catalysts[10] or metal-embedded mesoporous materials, such as MCM-41[3] and SBA-15,[11] were proven efficient in those epoxidation processes. For such catalytic systems, the presence of metals was believed to be pivotal for the construction of the active sites, which facilitate the adsorption and subsequent reaction for both the alkenes and oxidants.[12] Particularly, titanium-substituted silicalite (TS-1) was demonstrated to be very effective for styrene epoxidation, and the highly dispersed Ti species incorporated in the zeolitic matrix was identified as the key contributor of this catalytic activity.[13]

In addition to the reports on metal-based catalysts for alkene epoxidation, few studies have been published so far on the investigation of nonmetal catalysts. Recently, extensive studies have been carried out on graphene-based hybrid materials to investigate the potential applications of such materials in the fields of adsorption and catalysis. Metal-modified graphene hybrid materials have been widely used in oxygen reduction reactions,[14,15] batteries,[16] supercapacitors,[17] catalysis,[18] and photocatalysis.[19] Moreover, it has been reported that the electronic structure of graphene can be significantly modified by the introduction of certain heteroatoms, such as N[20] and B.[21] Therefore, their catalytic properties were altered as a consequence, which was also previously reported in carbon nanotube system for oxidative dehydrogenation of alkanes and carbon nitride system for cyclohexane oxidation.[22−24] Particularly, graphene and heteroatom-modified graphene were reported to be able to catalyze various catalytic reactions, such as hydrogenation, polymerization, alcohol oxidation, oxidative coupling, and even C−H bond activation.[25−33] However, until now, there has been no report on the catalytic epoxidation of a double bond over a graphene catalyst. In this current study, we prepared N-containing few-layered graphene

Received: January 16, 2014
Revised: March 17, 2014
Published: March 19, 2014

   dx.doi.org/10.1021/cs500062s | *ACS Catal.* 2014, 4, 1261−1266

materials and a series of N-doped graphene/layered carbon materials by the high-temperature ammonia treatment method. It was observed that the epoxidation of *trans*-stilbene could be triggered over N-containing graphene catalysts. The catalyst is very stable and easily recycled. By XPS tests and other control experiments, we identified that the lattice nitrogen species that stayed at the graphitic site, instead of the iron dopant, is responsible for the epoxidation reaction.

On the basis of the temperatures at which NG samples were treated, they were denoted as NG-*x* (*x* stands for the temperature of treatment at 200, 400, 600, and 800 °C).

The XRD profiles of the graphite, NG and NG-*x* are shown in Figure 1a. In addition to graphite, all the other samples

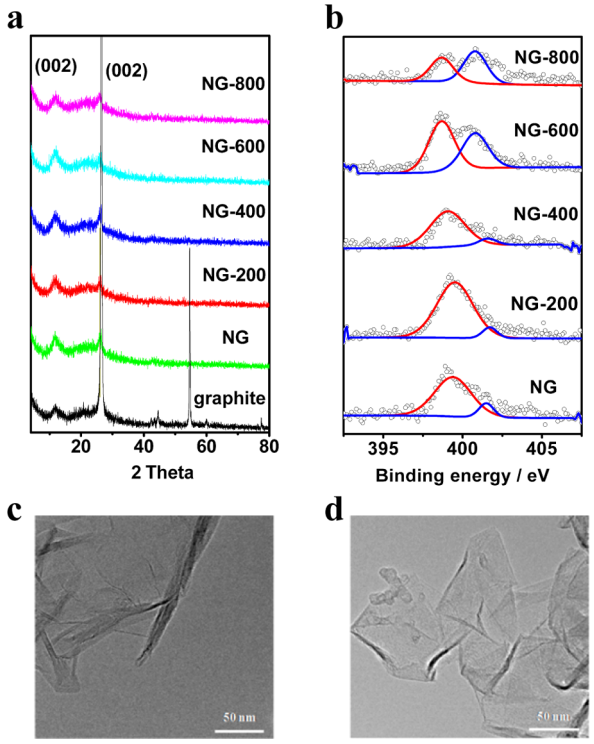

Figure 1. Characterization of catalysts. (a) XRD patterns of different catalysts; (b) XPS spectrum of N 1s in different catalysts; (c) TEM image of NG; (d) TEM image of NG-800.

exhibit two well-resolved reflections at 11.6° and 26.4° (2θ). The former signal suggests lamellar structure with a *d*-spacing of 0.7 nm. Compared with that of the pristine graphite, the intensity of the reflection at 26.4° decreases as a result of the poorer crystallinity caused by the swelling of graphene sheets. The morphology of NG and NG-*x* was determined by transmission electron microscopy (TEM, SEM) method (Figure 1c,d and Supporting Information, Figure S1a–c,e,f). TEM of NG showed randomly aggregated, crumpled sheets with a relatively large size distribution (from around 100 nm to few micrometers). After the introduction of nitrogen, the morphology of graphene sheets did not exhibit noticeable differences under TEM observations, as shown in Figure 1d.

The epoxidation of *trans*-stilbene was conducted at 373 K in a glass pressure vessel, with CH_2Cl_2 as the solvent and TBHP (65% in water) as the oxidant. The *trans*-stilbene epoxide was the main epoxidation product, with benzaldehyde as the byproduct possibly resulting from the oxidative cleavage of the double bond in *trans*-stilbene. When N-doped graphene with very low nitrogen concentration (0.48%) was used as the catalyst, a conversion of 3.8% could be reached in 1 h, and the selectivity toward epoxide was 80.9% (Table 1, entry 1). After

Table 1. Epoxidation of Alkenes on Different Catalysts[a]

					selectivity (%)[d]	
entry	catalyst	N (%)[b]	Fe (ppm)[c]	conv (%)[d]	epoxide	benzaldehyde
1[e]	NG	0.48	323	3.8	80.9	19.1
2[e]	NG-200	0.58	377	6.0	87.0	13.0
3[e]	NG-400	1.29	289	11.1	89.7	10.3
4[e]	NG-600	0.66	347	25.1	86.4	13.6
5[e]	NG-800	0.42	373	25.5	85.8	14.2
6[f]	NG-800	0.42	373	95.8	94.5	5.5
7[g]	NG-800	0.42	373	94.8	93.5	6.5
8[h]	1%Fe/NG-800	0.42	1%	23.1	91.8	8.2
9[i]	NG	0.48	323	54.5	87.5	12.5
10[i]	NG-800	0.42	373	87.6	72.8	27.2

[a]Reaction conditions: substrate (1 mmol), catalyst (10 mg), TBHP (3 mmol), urea (3 mmol), CH_2Cl_2 (2 mL), water (1 mL), *T* = 373 K. [b]Determined by elemental analysis. [c]Determined by ICP. [d]GC yield. [e]*trans*-Stilbene as substrate, *t* = 1 h. [f]*trans*-Stilbene as substrate, *t* = 24 h. [g]*trans*-Stilbene as substrate, 10 mg KCN was added, *t* = 24 h. [h]$Fe(NO_3)_3$ as precursor, calcined at 150 °C for 4 h under nitrogen flow. [i]Styrene as the substrate, *t* = 24 h.

treating NG with ammonia at 200 °C (NG-200), more nitrogen atoms were incorporated into the structure of graphene. We then observed an increase in catalytic activity (with conversion of 6.0%), and a slight increase in selectivity toward epoxide (87.0%). This demonstrated that ammonia treatment of the graphene is beneficial to its epoxidation reactivity.

The catalytic activity increases with treatment temperature (Table 1, entry 3). Significantly, for the NG sample treated with ammonia at 600 °C, a drastic improvement in its catalytic performance was observed (Table 1, entry 4), that is, the selectivity toward epoxide reached 86.4% while the conversion reached 25.1%. When the treating temperature ramped up to 800 °C, the catalyst thus prepared still exhibited a high catalytic performance comparable to that of NG-600 catalyst (Table 1, entry 5). When prolonging the reaction time to 24 h, the conversion of *trans*-stilbene over NG-800 catalyst can be as high as 95.8%, and the selectivity toward epoxide is around 95% (Table 1, entry 6). This demonstrated that by ammonia treatment at relatively high temperature, we could dramatically improve the catalytic performance of the N-doped graphene catalysts. With the increase in the ammonia treatment temperature (600 and 800 °C), a drop in the nitrogen concentration was observed (Table 1). For NG-600 and NG-800 catalysts, only 0.66% and 0.42 wt %, respectively, of nitrogen was observed by elemental analysis. This is almost one-half and one-third that of NG-400. One needs to note that at the same time, instead, the catalytic performance increased dramatically (Table 1, entries 3–5).

To understand the phenomenon, the states of N in the materials were investigated by N 1s XPS. Depending on their location in the graphene sheets, nitrogen can be classified into pyrrolic N, pyridinic N, amine groups N, and quaternary N.[34−36] For pristine NG, most of the nitrogen stays as pyridinic N or amine groups (399.3 eV, Figure 1b). Although the concentration of nitrogen increased for NG-200 and NG-400, their N 1s XPS profiles maintained a shape similar to that of

dx.doi.org/10.1021/cs500062s | *ACS Catal.* 2014, 4, 1261−1266

NG, indicating that most of the nitrogen is pyridinic N or amine groups. For NG-600 and NG-800, albeit the morphology of the samples did not change (Figure 1c,d and Supporting Information, Figure S1a–c), the distribution of nitrogen over graphene changed extensively. From Figure 1b, it is clear that the share of quaternary N increased dramatically over temperature, and for NG-800, it becomes the main peak of the spectrum. However, as from elemental analysis, an extensive loss of nitrogen was observed simultaneously.

Reasonably, at relatively high treatment temperature, the distribution of nitrogen in graphene was governed by the balance between nitrogen removal/doping due to the high temperature treatment and/or the reconstruction of nitrogen among different sites. The NG-600 and NG-800 that have the relatively low concentration of nitrogen dopant but the highest population of quaternary N possess the best epoxidation catalytic performance. Indeed, when we tried to correlate the catalytic activity with the concentration of quaternary N in the catalyst, we observed a linear relationship between the graphitic nitrogen concentration and the activity (Figure 4). These results demonstrated very clearly that the quaternary N is responsible for the high epoxidation activity observed on ammonia-treated NG materials. In addition, NG and NG-800 were also investigated for the epoxidation reaction of styrene. The results are listed in Table 1 (entries 9 and 10), suggesting that NG-800 was very efficient in catalyzing the epoxidation of styrene, as well.

The reaction behavior of the epoxidation of *trans*-stilbene over NG-800 under different conditions was investigated (Figure 2; Supporting Information, Table S1). The yield of *trans*-stilbene epoxide was 21.9% within the first hour and gradually increased to 84.3% with the reaction running for 12 h. A slight increase in the conversion and selectivity to *trans*-stilbene epoxide was observed when the reaction ran for a longer time. At the same time, it was interesting to note that the selectivity of benzaldehyde dropped with the progress of the reaction while its yield remained at a relatively constant level for 24 h (Figure 2c). This result suggests that in the induction period of the reaction, the oxidative C–H bond cleavage coexisted with the epoxidation process. However, with the reaction going on, the epoxidation was the dominant reaction and the formation of benzaldehyde was suppressed.

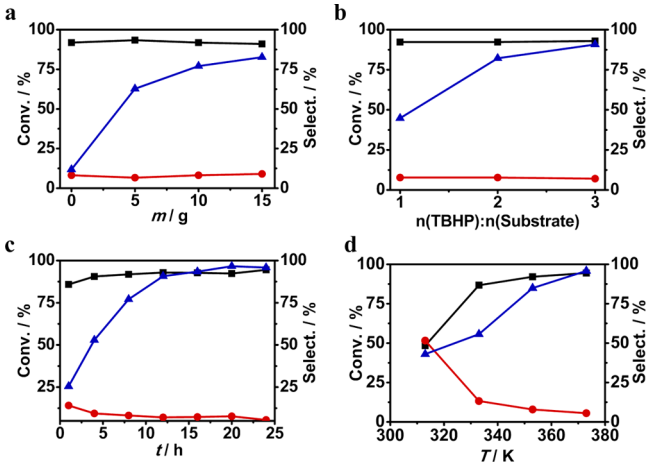

Figure 2. Catalytic activity and selectivity of NG-800 on the epoxidation of *trans*-stilbene under different conditions. (a) Effect of the amount of catalyst, TBHP (3 mmol), T = 373 K, t = 8 h; (b) effect of the amount of TBHP, NG-800 (10 mg), T = 373 K, t = 12 h; (c) effect of reaction time, NG-800 (10 mg), TBHP (3 mmol), T = 373 K; (d) effect of reaction temperature, NG-800 (10 mg), TBHP (3 mmol), t = 24 h. Reaction conditions: *trans*-stilbene (1 mmol), urea (3 mmol), CH_2Cl_2 (2 mL), water (1 mL). Symbols: blue triangle, conversion of *trans*-stilbene; black square, selectivity to *trans*-stilbene epoxide; red dot, selectivity to benzaldehyde.

Figure 2d illustrates the conversion of *trans*-stilbene and the selectivity to products with temperature. Clearly, the epoxidation reaction is favored at higher reaction temperature. The catalyst is very stable and maintains a high catalytic performance via a stability check by reusing the NG-800 catalyst seven times. As illustrated in Figure 3, the catalytic

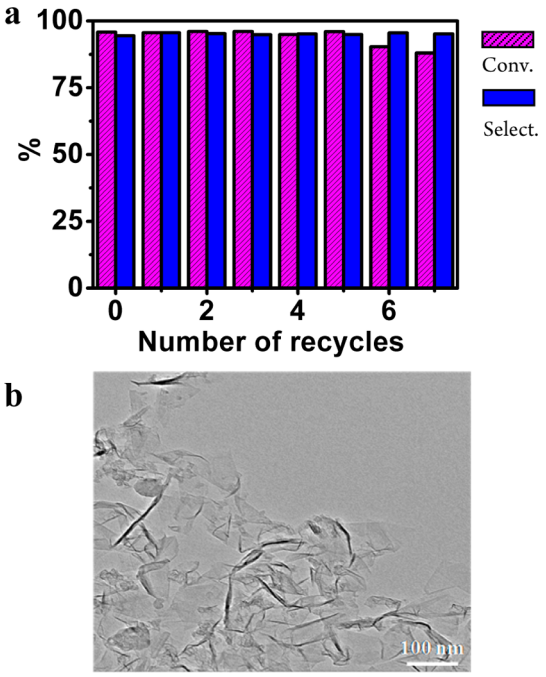

Figure 3. (a) Recycling studies of NG-800 on *trans*-stilbene epoxidation. Conv. means conversion of *trans*-stilbene; Select. means selectivity toward epoxidation product. Reaction conditions: *trans*-stilbene (1 mmol), NG-800 (10 mg), urea (3 mmol), CH_2Cl_2 (2 mL), water (1 mL), T = 373 K, t = 24 h. (b) TEM picture of NG-800 after first use.

activity of NG-800 on the epoxidation of *trans*-stilbene remains almost unchanged during the first five runs (95%), and it dropped only slightly after seven recycles, but the selectivity always stayed at a constant level (95%). The catalyst kept the same morphology with previous NG-800 after reaction. These results strongly indicate that nitrogen-doped graphene is a very active and stable catalyst for the epoxidation reaction.

We then come to the question why this catalyst is so active in the epoxidation reaction. On the basis of elemental analysis (EA) and XPS and ICP results, we noticed that, in addition to carbon and nitrogen, the pristine NG and those after ammonia treatment all contain an impurity of iron (determined by ICP). As shown in Table 1, NG and NG-x contain around 350 ppm Fe, indicating the content of iron in all the tested catalysts is relatively constant and independent of ammonia treatment. However, we observed that NG contains 0.48% nitrogen, and treating this material with ammonia at 200 °C and then at 400 °C will bring the concentration of nitrogen up to 1.29% for the NG-400 catalyst. Most of these newly incorporated nitrogen

dx.doi.org/10.1021/cs500062s | *ACS Catal.* 2014, 4, 1261–1266

atoms stayed at the graphitic sites (Figure 1b; Supporting Information, Figure S2b). More importantly, the yield of epoxide is in line with the concentration of graphitic nitrogen in these samples (Figures 1b, 4). This result suggests that

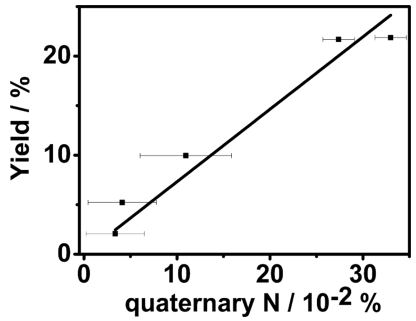

Figure 4. The relationship between the catalytic activity (yield of stilbene epoxide) and the concentration of quaternary nitrogen in the N-doped graphene catalysts.

graphitic nitrogen is critical for the epoxidation reaction, which is in good agreement with previous reports that nitrogen incorporation can stimulate the chemical reactivity of adjacent carbon species, making it an active catalyst for oxidation reactions.[31] However, because iron and nitrogen coexist on all those catalytically active samples, it is unclear whether it was iron or nitrogen alone or the combination of these two components that generated the epoxidation activity.

To check whether iron is critical for the epoxidation, we prepared the 1% Fe/NG-800 catalyst, where the concentration of iron is around 30 times of that of NG-800 (although the chemical state of iron may be different from those of fresh NG). As shown in Table 1 (entry 8), the conversion of stilbene and selectivity to epoxide are almost the same as that of parent NG-800. This result implies that the presence of iron alone is irrelevant to the epoxidation activity. This conclusion is also confirmed by the fact that although NG, NG-600, and NG-800 have similar iron contents, they exhibited a huge difference in reaction activity. To verify this conclusion, we prepared three pristine NG catalysts, each containing the same amount of nitrogen and different amounts of iron impurity (Supporting Information, Table S2 and Figure S3). The reaction results show that the catalytic performance is not in line with the content of iron impurity and confirm that iron alone is not the center for the catalytic epoxidation reaction.

Is it possible that iron and graphitic nitrogen function synergistically to generate the catalytic active center? It has been reported that Pd nanoparticles supported on nitrogen-doped nanoporous carbon could be bound to nitrogen atoms incorporated in carbon to enhance the catalytic activity of hydrocarbon and alcohol oxidation.[37] Furthermore, over nitrogen-doped CNT-based catalysts, the iron impurity cooperates with the nitrogen to form structures containing an iron−nitrogen bond as well as Fe−N proximity. These iron/nitrogen species were believed to be responsible for the good activity in the oxygen reduction reaction.[14] To determine whether this also happens in the current study, NG-800 was used to investigate the epoxidation reaction with 10 mg KCN added into the reaction system. Because CN^- can coordinate strongly with iron and consequently poison the iron-centered catalytic sites, if iron alone or the Fe−N moiety is the active center for epoxidation reaction, the catalytic performance should be observed with a remarkable decrease with the addition of KCN. However, the reaction activity remains almost the same after CN^- is added (Table 1, entry 7). This implies that the catalytic activity of these materials is not affected by the iron element, although it exists in all catalysts at different contents.

Our previous report on the study of selective oxidation of ethylbenzene with nitrogen-doped sp^2-hybridized carbon by using the soft X-ray adsorption technique suggests that it is the graphitic nitrogen dopant that modulated the electronic structure of sp^2 carbon material. The density of states intensities near the Fermi level for the adjacent ortho-carbon are much stronger than those of undoped graphene carbon, which confers the nitrogen-neighboring carbon a metallike d band electronic structure and makes the adjacent carbon more capable to host the formation of reaction oxygen species; the peroxide; and, consequently; to activate saturated hydrocarbon. We believe that this is also the case in the current study because the presence of graphitic nitrogen dopant is responsible for the observed epoxidation activity; that is, the catalytic performance is in line with the concentration of graphitic nitrogen in those nitrogen-doped sp^2 carbon materials (Figure 4).

To better understand the mechanism of the outstanding catalyic activity of the nitrogen-doped sp^2 carbon catalyst and the oxidation of the carbon−carbon double bonds, we report here the density functional theory (DFT) calculations using opt88 functionals. As shown in Figure 5, the ortho-carbon in

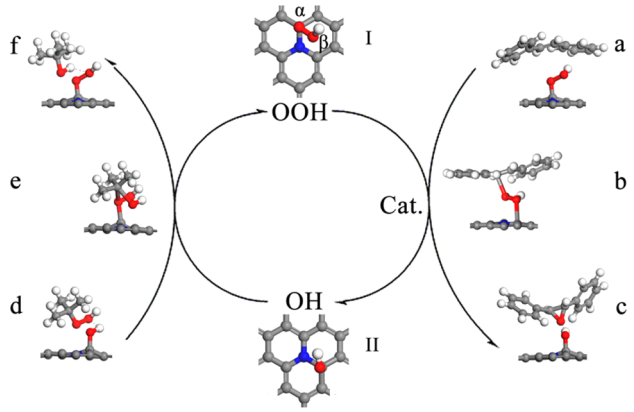

Figure 5. The reaction mechanism for the epoxidation of *trans*-stilbene on nitrogen-doped graphene catalyst.

nitrogen-doped graphene is the most stable adsorption site of peroxide-like species,[31,38,39] OOH. The α-oxygen (that does not connect with hydrogen) in the pristine reactive oxygen species stays straight above one of the ortho-carbons, and the β-oxygen atom is pointing toward another ortho-carbon around the graphitic nitrogen (Figure 5I). Because graphene has a big π system, reactants with π orbitals such as stilbene or styrene are able to adsorb on its surface via a strong $\pi-\pi$ interaction (Figure 5a).[40,41] With the benzene rings stabilized by the graphene domain, the locked internal C−C double bond lies on top of reactive oxygen species with a favorite adsorption energy of −0.43 eV.

In the transition state (Figure 5b), the carbon−carbon double bond is attacked by the α-oxygen of the reactive oxygen species. Because of the existence of three equivalent ortho-carbons (Supporting Information, Figure S4), the reaction between the α-oxygen with and the double bond, the oxygen−oxygen bonds were elongated while the terminal hydroxyls

dx.doi.org/10.1021/cs500062s | ACS Catal. 2014, 4, 1261−1266

containing the β-oxygen were hopping toward another adjacent ortho-carbon, which is positively charged (average 0.21 eV) and with delocalized spin density. As a result, the epoxide is formed (Figure 5c), and the terminal hydroxyls jumped and were accommodated on the adjacent ortho-carbon (Figure 5c, II). The reaction is exothermic (−1.85 eV) with a moderate barrier of 0.61 eV. Significantly, the surface reactive oxygen species can be recovered by the reaction between TBHP and the surface hydroxyls groups (with a barrier of 0.5 eV, Figure 5d-f), which completed the reaction cycle. It is worth noting that the three ortho-carbons around the center nitrogen atom are equivalent in geometric and electronic properties. Although the formation of reactive oxygen species was governed by the modulated electronic structure of the N-doped graphene catalysts, the unique geometric feature described here renders the epoxidation, particularly the transferring/hopping of hydroxyls and the successive recycling of the reactive oxygen species, possible. This is pivotal for the current metal-free epoxidation reaction system.

In conclusion, nitrogen-doped graphene catalysts synthesized through a simple ammonia high-temperature treatment method were demonstrated to be very active for the C−C double bond epoxidation reaction. It is the unique property of the nitrogen dopants at the quaternary site that confers the material the outstanding catalytic activity. This is the first report of the epoxidation reaction using nonmetal, graphene-based catalytic systems, which, once fully developed, is believed to be a very promising invention as an alternative technology to the metal-based catalysts.

■ ASSOCIATED CONTENT

Supporting Information

Experimental procedures, the effects of different reaction conditions, as well as the iron impurity on the epoxidation catalytic activity. Figures S1−S4 and Tables S1−S2. This material is available free of charge via the Internet at http://pubs.acs.org."

■ AUTHOR INFORMATION

Corresponding Authors

*Phone: +86-571-88871037. Fax: +86-571-88871037. E-mail: jgw@zjut.edu.cn.

*Phone: +86-10-62758603. Fax: +86-10-62758603. E-mail: dma@pku.edu.cn.

Notes

The authors declare no competing financial interest.

■ ACKNOWLEDGMENTS

This work received financial support from the 973 Project (2013CB933100, 2011CB201402, 2013CB733501) and Natural Science Foundation of China (21173009, 21222306, 91334013).

■ REFERENCES

(1) Pavel, O. D.; Cojocaru, B.; Angelescu, E.; Pârvulescu, V. I. *Appl. Catal., A* **2011**, *403*, 83−90.

(2) Murphy, A.; Dubois, G.; Stack, T. D. P. *J. Am. Chem. Soc.* **2003**, *125*, 5250−5251.

(3) Zhang, Q. H.; Wang, Y.; Itsuki, S.; Shishido, T.; Takehira, K. *J. Mol. Catal. A: Chem.* **2002**, *188*, 189−200.

(4) Lignier, P.; Morfin, F.; Mangematin, S.; Massin, L.; Rousset, J. L.; Caps, V. *Chem. Commun. (Cambridge)* **2007**, 186−188.

(5) Qi, B.; Lu, X. H.; Zhou, D.; Xia, Q. H.; Tang, Z. R.; Fang, S. Y.; Pang, T.; Dong, Y. L. *J. Mol. Catal. A: Chem.* **2010**, *322*, 73−79.

(6) Mandelli, D.; Vliet, M. C. A.; Sheldon, R. A.; Schuchardt, U. *Appl. Catal., A* **2001**, *219*, 209−213.

(7) Gelalcha, F. G.; Bitterlich, B.; Anilkumar, G.; Tse, M. K.; Beller, M. *Angew. Chem., Int. Ed.* **2007**, *46*, 7293−7296.

(8) Ding, Z. X.; Chen, X. F.; Antonietti, M.; Wang, X. C. *ChemSusChem.* **2011**, *4*, 274−281.

(9) Schröder, K.; Join, B.; Amali, A. J.; Junge, K.; Ribas, X.; Costas, M.; Beller, M. *Angew. Chem., Int. Ed.* **2011**, *50*, 1425−1429.

(10) Patil, N. S.; Uphade, B. S.; Jana, P.; Bharagava, S. K.; Choudhary, V. R. *J. Catal.* **2004**, *223*, 236−239.

(11) Tang, Q. H.; Hu, S. Q.; Chen, Y. T.; Guo, Z.; Hu, Y.; Chen, Y.; Yang, Y. H. *Microporous Mesoporous Mater.* **2010**, *132*, 501−509.

(12) Zhan, W. C.; Guo, Y. L.; Wang, Y. Q.; Guo, Y.; Liu, X. H.; Wang, Y. S.; Zhang, Z. G.; Lu, G. Z. *J. Phys. Chem. C* **2009**, *113*, 7181−7185.

(13) Zhuang, J. Q.; Yang, G.; Ma, D.; Lan, X. J.; Liu, X. M.; Han, X. M.; Bao, X. H.; Mueller, U. *Angew. Chem., Int. Ed.* **2004**, *43*, 6377−6381.

(14) Li, Y. G.; Zhou, W.; Wang, H. L.; Xie, L. M.; Liang, Y. Y.; Wei, F.; CarlosIdrobo, J.; Pennycook, S. J.; Dai, H. J. *Nat. Nanotechnol.* **2012**, *7*, 394−400.

(15) Liang, Y. Y.; Li, Y. G.; Wang, H. L.; Zhou, J. G.; Wang, J.; Regier, T.; Dai, H. J. *Nat. Mater.* **2010**, *10*, 780−786.

(16) Wang, H. L.; Yang, Y.; Liang, Y. Y.; Zheng, G. Y.; Li, Y. G.; Cui, Y.; Dai, H. J. *Energy Environ. Sci.* **2012**, *5*, 7931−7935.

(17) Wang, H. L.; Casalongue, H. S.; Liang, Y. Y.; Dai, H. J. *J. Am. Chem. Soc.* **2010**, *132*, 7472−7477.

(18) Gao, Y. J.; Ma, D.; Hu, G.; Zhai, P.; Bao, X. H.; Zhu, B.; Zhang, B. S.; Su, D. S. *Angew. Chem., Int. Ed.* **2011**, *50*, 10236−10240.

(19) Liang, Y. Y.; Wang, H. L.; Casalongue, H. S.; Chen, Z.; Dai, H. J. *Nano Res.* **2010**, *3*, 701−705.

(20) Wang, X. R.; Li, X. L.; Zhang, L.; Yoon, Y.; Weber, P. K.; Wang, H. L.; Guo, J.; Dai, H. J. *Science* **2009**, *324*, 768−771.

(21) Zhao, M.; Huang, Y. H.; Ma, F.; Hu, T. W.; Xu, K. W.; Chu, P. K. *J. Appl. Phys.* **2013**, *114*, 063707.

(22) Zhang, J.; Liu, X.; Blume, R.; Zhang, A. H.; Schlögl, R.; Su, D. S. *Science* **2008**, *322*, 73−77.

(23) Frank, B.; Zhang, J.; Blume, R.; Schlögl, R.; Su, D. S. *Angew. Chem., Int. Ed.* **2009**, *48*, 6913−6917.

(24) Wang, Y.; Zhang, J. S.; Wang, X. C.; Antonietti, M.; Li, H. R. *Angew. Chem., Int. Ed.* **2010**, *49*, 3356−3359.

(25) Gao, Y. J.; Ma, D.; Wang, C. L.; Guan, J.; Bao, X. H. *Chem. Commun.* **2011**, *47*, 2432−2434.

(26) Dreyer, D. R.; Jarvis, K. A.; Ferreira, P. J.; Bielawski, C. W. *Polym. Chem.* **2012**, *3*, 757−766.

(27) Dreyer, D. R.; Jarvis, K. A.; Ferreira, P. J.; Bielawski, C. W. *Macromolecules* **2011**, *44*, 7659−7667.

(28) Dreyer, D. R.; Jia, H. P.; Bielawski, C. W. *Angew. Chem., Int. Ed.* **2010**, *49*, 6813−6816.

(29) Long, J. L.; Xie, X. Q.; Xu, J.; Gu, Q.; Chen, L. M.; Wang, X. X. *ACS Catal.* **2012**, *2*, 622−631.

(30) Li, X. H.; Antonietti, M. *Angew. Chem., Int. Ed.* **2013**, *52*, 4572−4576.

(31) Gao, Y. J.; Hu, G.; Zhong, J.; Shi, Z. J.; Zhu, Y. S.; Su, D. S.; Wang, J. G.; Bao, X. H.; Ma, D. *Angew. Chem., Int. Ed.* **2013**, *52*, 2109−2133.

(32) Jia, H. P.; Dreyer, D. R.; Bielawski, C. W. *Tetrahedron* **2011**, *67*, 4431−4434.

(33) Yang, J. H.; Sun, G.; Gao, Y. J.; Zhao, H. B.; Tang, P.; Tan, J.; Lu, A. H.; Ma, D. *Energy Environ. Sci.* **2013**, *6*, 793−798.

(34) Li, X. L.; Wang, H. L.; Robinson, J. T.; Sanchez, H.; Diankov, G.; Dai, H. J. *J. Am. Chem. Soc.* **2009**, *131*, 15939−15944.

(35) Lin, C. Y.; Lin, C. Y.; Chiu, P. W. *Appl. Phys. Lett.* **2010**, *96*, 133110 (1−3).

(36) Sharifi, T.; Hu, G. Z.; Jia, X. E.; Wagberg, T. *ACS Nano* **2012**, *6*, 8904−8912.

(37) Zhang, P. F.; Gong, Y. T.; Li, H. R.; Chen, Z. R.; Wang, Y. *Nat. Commun.* **2013**, *4*, 1593 (1−11).
(38) Zheng, Y.; Jiao, Y.; Ge, L.; Jaroniec, M.; Qiao, S. Z. *Angew. Chem., Int. Ed.* **2013**, *52*, 3110−3116.
(39) Zhong, X.; Yu, H. Y.; Zhuang, G. L.; Li, Q.; Wang, X. D.; Zhu, Y. S.; Liu, L.; Li, X. N.; Dong, M. D.; Wang, J. G. *J. Mater. Chem. A* **2014**, *2*, 897−901.
(40) Gao, Y. J.; Hu, G.; Zhang, W.; Ma, D.; Bao, X. H. *Dalton Trans.* **2011**, *40*, 4542−4547.
(41) Yang, J. H.; Gao, Y. J.; Zhang, W.; Tang, P.; Tan, J.; Lu, A. H.; Ma, D. *J. Phys. Chem. C* **2013**, *117*, 3785−3788.